PROGRESSIVE WAVE EFFECTS ON BOUNDARY LAYER FLOW AND SHEET-FLOW SEDIMENT TRANSPORT

Wouter Kranenburg[1], Jan Ribberink[2]

Abstract

In the near-shore zone, energetic surface waves generate sheet-flow sand transport. The progressive nature of the waves also induces an onshore directed current near the bed. This paper investigates numerically the influence of this current and other progressive wave effects on wave boundary layer flow and sheet-flow sand transport. The resulting insights and parameterizations facilitate further improvement of sand transport formulas. This is relevant, because transport formulas are mainly based on oscillatory flow experiments which do not include progressive wave effects.

Key words: wave boundary layer, wave-induced currents, sheet-flow, sediment transport, numerical modeling

1. Introduction

In morphodynamic models, wave-induced sediment transport is usually predicted with semi-empirical transport formulas. These formulas are largely based on experiments in *oscillatory flow tunnels*, laboratory facilities in which the near bed water motion is physically modeled with horizontally uniform oscillating flow. In these experiments much attention has been given to the sheet-flow transport regime, where bed forms are washed away and the bed is turned into a moving sediment layer (Ribberink et al., 2008). This has resulted in insights in e.g. the effect of the wave shape and the grain size on bed shear stresses and sediment transport rates, which has been incorporated in the sediment transport formulas through parameterizations. An important insight from sheet-flow experiments in tunnels is that under velocity-

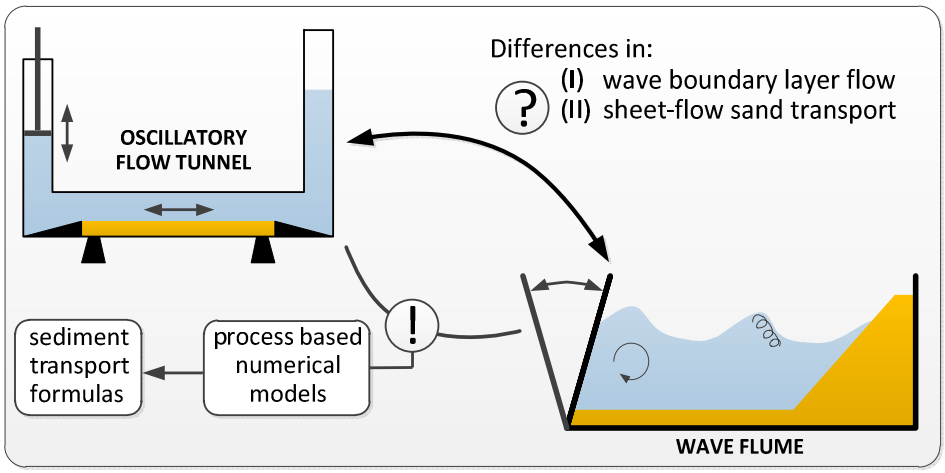

Figure 1. Graphical summary

[1] Water Engineering and Management, University of Twente, P.O. Box 217, 7500 AE Enschede, The Netherlands. w.m.kranenburg@utwente.nl
[2] Water Engineering and Management, University of Twente, P.O. Box 217, 7500 AE Enschede, The Netherlands. j.s.ribberink@utwente.nl

skewed flow (present under waves with amplified crests like Stokes waves) the transport of coarse grains is mainly in onshore direction, but that net transport decreases with decreasing grain sizes and can even become negative (O'Donoghue & Wright, 2004). This is explained by the phase-lag effect: fine sediment, stirred up by the strong onshore flow, settles only slowly and is therefore still partly suspended during flow reversal and subsequently transported offshore during the offshore flow (Dohmen-Janssen et al., 2002).

The rationale for this study is that recent sheet-flow experiments in large scale wave flumes, with progressive wave instead of oscillatory flow, show increased transport in onshore direction compared to the earlier experiments in tunnels (Dohmen-Janssen & Hanes, 2002). For Stokes waves over fine sediments, this even includes a reversal of the net transport direction from offshore (tunnel) to onshore (flume) (Schretlen, 2012): apparently the phase-lag effects are canceled out by effects of wave progression. An important question is therefore: what are the effects of wave progression on boundary layer flow and sheet-flow sediment transport? Insight herein can help to improve existing sediment transport formulas which is relevant for morphological modeling.

A wave progression effect potentially explaining the increased onshore transport in flumes is *progressive wave streaming*. This is an onshore directed bottom boundary layer current generated under influence of the vertical orbital motions beneath progressive waves (Longuet-Higgins, 1953). The mechanism works as follows: bed shear stress and boundary layer turbulence cause the horizontal motion inside the wave boundary layer (WBL) to run in front compared to the free stream (FS) velocity. Through continuity, this causes also a phase lead in the vertical velocity at the upper edge of the boundary layer. As a result, horizontal and vertical motion at that level are more than 90^o out of phase. This introduces a wave-averaged transport of horizontal momentum towards the bed that drives the onshore current (Figure 2a). Note that this process acts opposite to *wave shape streaming* (Trowbridge & Madsen, 1984), a mechanism that can be present both in tunnels and flumes. Wave shape streaming is the result of differences in time-dependent bed shear stress and turbulence between the on- and offshore water motion under non-sinusoidal waves/oscillations. This causes a non-zero wave-averaged turbulent shear stress, driving an offshore directed current (Figure 2b).

In this paper we determine the importance of progressive wave streaming for wave-induced boundary layer flow, and investigate whether this mechanism is the full explanation of the observed flume-tunnel difference in sediment transport. Section 2 briefly discusses the numerical model developed and applied in this study. Section 3 focusses on the boundary layer flow, discussing successively results of validation tests, numerical tests on the importance of streaming and parameterization hereof. Section 4 follows the same structure, but then focusing on sediment transport. Section 5 briefly discusses the potential implications of our results for morphological modeling. The conclusions are summarized in section 6.

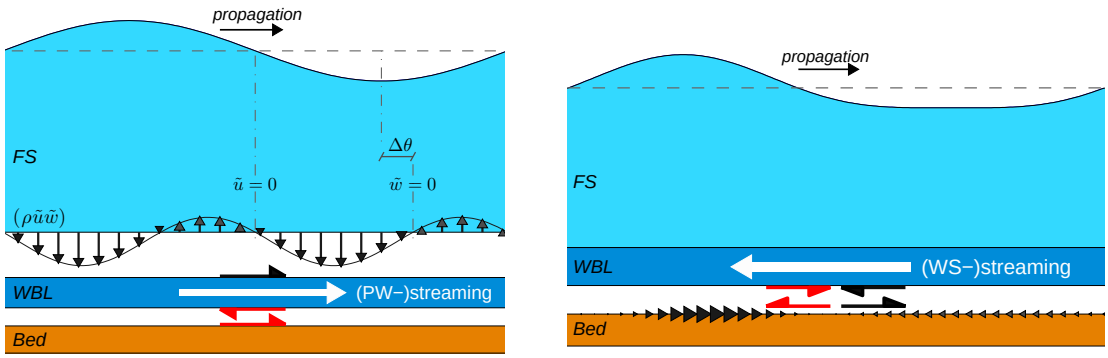

Figure 2. Schematic drawing of boundary layer streaming mechanisms; (a) Progressive Wave Streaming; (b) Wave Shape Streaming; Small black arrows: wave-generated momentum transport (a) or bed shear stress (b); Black shear arrows: resulting wave-averaged stress; White arrow: generated current; Red shear arrows: current-related bed shear stress.

2. Model

Our model can be classified as a 1DV Reynolds Averaged Navier-Stokes (RANS) flat bed boundary layer model with k-ε turbulence closure and an advection-diffusion formulation for suspended sediment. The fundamental unknowns solved by the model are horizontal flow velocity u, vertical flow velocity w, sediment concentration c and turbulent kinetic energy k and its rate of dissipation ε. The flow velocities are solved from the following (reduced) momentum and continuity equation:

$$\frac{\partial u}{\partial t}+u\frac{\partial u}{\partial x}+w\frac{\partial u}{\partial z}=-\frac{1}{\rho_w}\frac{\partial p}{\partial x}+\frac{\partial}{\partial z}\left\{(\upsilon+\upsilon_t)\frac{\partial u}{\partial z}\right\} \tag{1}$$

$$\frac{\partial u}{\partial x}+\frac{\partial w}{\partial z}=0 \tag{2}$$

where p the pressure, ρ_w the fluid density, υ the kinematic viscosity of water, υ_t the turbulence viscosity, x and z the horizontal and vertical coordinate, positive in onshore and upward direction respectively. The closure for υ_t is provided by the k-ε turbulence model. Hereby $\upsilon_t = c_\mu k^2/\boldsymbol{\varepsilon}$ with k and ε respectively the turbulent kinetic energy and its dissipation rate and c_μ a constant. The model accounts for conversion of turbulent kinetic energy to potential energy with the mixing of sediment. This is included in the model through a buoyancy flux term, basically an additional energy loss term added to the standard clear fluid turbulence model.

The sediment (volume) concentration c is solved from a sediment balance:

$$\frac{\partial c}{\partial t}+u\frac{\partial c}{\partial x}+w\frac{\partial c}{\partial z}=\frac{\partial w_s c}{\partial z}+\frac{\partial}{\partial z}\left\{\left(\upsilon+\frac{\upsilon_t}{\sigma_t}\right)\frac{\partial c}{\partial z}\right\} \tag{3}$$

where we apply Prandtl-Schmidt number $\sigma_t = 0.7$. The local sediment fall velocity w_s is determined using the undisturbed settling velocity $w_{s,0}$ according Van Rijn (1993), with a correction for hindered settling in high sediment concentrations following Richardson & Zaki (1954).

A key element in the model is the assumption of uniform wave shape and height during propagating over the horizontal sand bed. Because of this the 2DV-model equations can be solved in a 1DV-model structure by transformation of horizontal gradients of velocity, turbulence properties and sediment concentration into time derivatives, using:

$$\frac{\partial ...}{\partial x}=-\frac{1}{c_p}\frac{\partial ...}{\partial t} \tag{4}$$

where c_p is the wave propagation speed.

Progressive wave effects are included in this model by the presence of advective transport of horizontal momentum, turbulence properties and sediment (see 2nd and 3rd term in equation 1 & 3). This marks the fundamental difference between modeling the horizontally uniform situation like in oscillating flow tunnels or the horizontally non-uniform situation in prototype situation and wave flumes. Switching off these terms reduces the model to a tunnel-model.

The model can be forced in two ways. We can either force the principally unknown $u(t,z)$ to match a predefined horizontal velocity signal at a certain vertical level, e.g. a measured time-series. In this case, the associated (oscillating plus mean) pressure gradient is determined iteratively every time step from equation (1) at the matching level. Alternatively, the oscillating horizontal pressure gradient can be determined in advance from a given free stream horizontal velocity $\tilde{u}_\infty$ with zero mean, e.g. from Stokes theory. In the latter approach the model does not account for a mass transport compensating return flow and the mean current is governed by the streaming mechanisms only.

The flow equation is solved using a no shear flow boundary condition at the top of the domain and a partial slip condition at the (rough) bed. For the sediment balance we use a no-flux condition at the top boundary and a pick-up function at reference height $z = z_a = 2d_{50}$. Representative model settings are: a time

step of 1/1000 times the wave period, a simulation length of 50 waves and a grid with 150 layers exponentially divided over 1.2 times the estimated boundary layer thickness. For more details, we refer to Kranenburg et al. (2012).

3. Results (I): Flow

3.1. *Validation results for net currents in the wave boundary layer*

Concerning the hydrodynamics, the model has been validated against intra-wave measurements of the boundary layer flow. Hereby, typical boundary layer characteristics like velocity overshoot, phase lead and the BL-thickness are reproduces very well. Because of our interest in the role of streaming in explaining the differences in sediment transport between the flume and tunnel experiments, we focus here on the validation results for the wave-averaged current. Figure 3 shows model results and data for three different experimental cases. The first case, from Klopman (1994), is a small-scale flume experiment of a nearly sinusoidal wave over a fixed bed. The second case, from Campbell et al. (2007), shows the net current for a tunnel experiment with velocity-skewed oscillatory flow over a fixed bed. The third case stems from the large scale flume experiments on sheet-flow sediment transport under velocity-skewed waves by Schretlen (2012). These conditions have been chosen to validate the model for a case with respectively progressive wave streaming, wave shape streaming, and both processes simultaneously. In all three cases, the model has been forced with a velocity signal measured outside the boundary layer. The subsequent model data comparison beneath that point shows that the model clearly captures the main features of the measured data, i.e. flow direction, velocity magnitude and profile shape. Note e.g. the onshore current in Figure 3a, the offshore current in Figure 3b and the location and magnitude of the local maximum/minimum in Figure 3c. The model-data comparison is not perfect, especially close to the bed. For case 1 (panel a) this might be explained by the influence of the individual roughness elements, which were relatively large because of the small-scale of this experiment. For case 3 (panel c), the reason is the unequal erosion of the mobile bed during on- and offshore flow under the velocity-skewed wave, which is not captured by the model. However, notwithstanding the differences, this validation shows that our model is able to capture the streaming phenomena, also when they are competing, as in case 3. For case 3, also a simulation has been added in which the progressive wave effects have been turned off. Comparison of the simulations shows the large influence of progressive wave streaming on the net current.

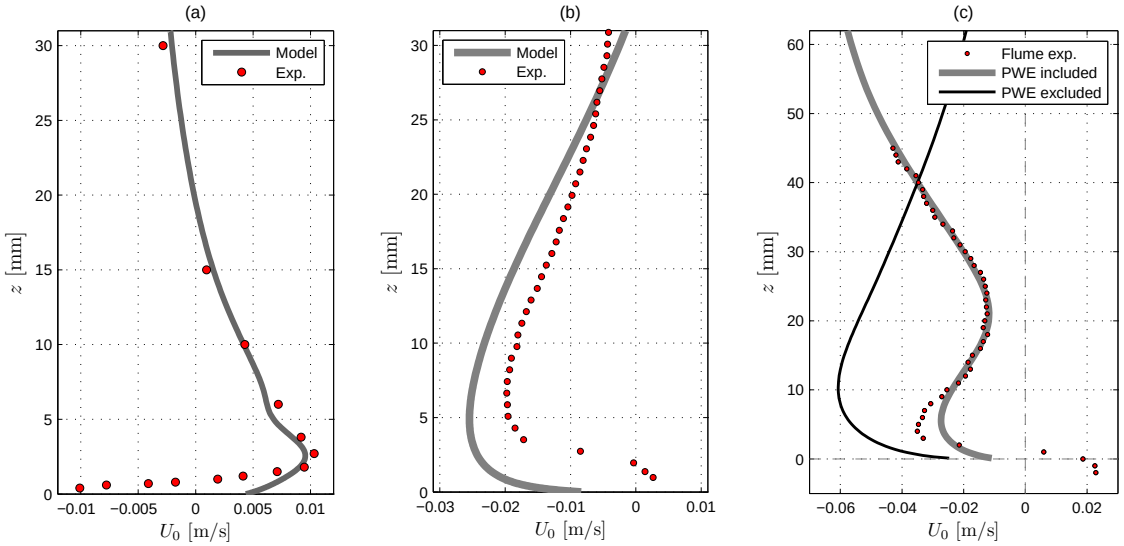

Figure 3. Model-data comparison on wave averaged velocity U_0 for (a) a sine wave in a small scale flume experiment, (b) a velocity-skewed oscillatory flow in a tunnel experiment, (c) a velocity-skewed wave in a large scale flume experiment.

3.2. *Results of model research on the relative importance of progressive wave streaming*

To get a more generic insight in the importance of progressive wave streaming compared to wave shape streaming, model tests have been carried out for various combinations of wave and bed parameters. Hereby, 2nd order Stokes wave theory has been applied to determine the near-bed free stream horizontal velocity. This signal has been used to force the model while the wave-averaged current was allowed to develop freely (so return currents are not considered). Using Stokes theory and considering turbulent boundary layers above fixed beds, the non-dimensional parameters $U_0 c/\hat{u}_1^2$, A/k_N and kh are sufficient to span the domain and describe the results. Hereby U_0 is the wave-averaged current, c the wave speed, $\hat{u}_1$ the amplitude of the first harmonic of the horizontal component of the free stream orbital velocity. A/k_N and kh denote the relative bed roughness and relative water depth respectively.

Figure 4b shows simulation results for the non-dimensional streaming velocity at the top of the boundary layer as function of kh. For a single parameter combination, also the vertical profile of the net current is shown (panel a). The results in panel b show a clear dependence on kh: streaming is positive at large kh, but decreases more and more for decreasing kh. The role of wave shape streaming and progressive wave streaming herein becomes clear from simulations with the separate streaming mechanisms only. Hereby, the contribution from wave shape streaming has been determined from simulations with identical forcing, but the advective terms of the momentum equation switched off (which reduces the test case to an oscillatory flow case). The contribution from progressive wave streaming has been found from simulations with the model forcing reduced to a sine wave only (only the first harmonic). This shows that at relatively deep water (large kh) the non-dimensional streaming is completely determined by the progressive wave streaming. For decreasing relative water depth (kh), the normalized progressive wave streaming stays nearly constant. However, the importance of wave shape effect relative to progressive wave streaming increases for decreasing water depth, resulting in a reversal from on- to offshore. In absolute sense, both effects increase while approaching the shore. However, wave shape streaming increases faster due to the changing wave shape. The existence of this balance has been discussed before (Trowbridge & Madsen, 1984). What is new here, is that is has been computed with a quantitatively validated numerical model. This allows for further quantification of the role of these mechanisms for sediment transport.

3.3. *Parameterization*

The numerical results on streaming have been parameterized. In this way, the results of the intra wave boundary layer model can be used to include progressive wave streaming and wave shape streaming into practical sand transport formulas, that either use a free stream velocity moment (Bagnold-Bailard type) or

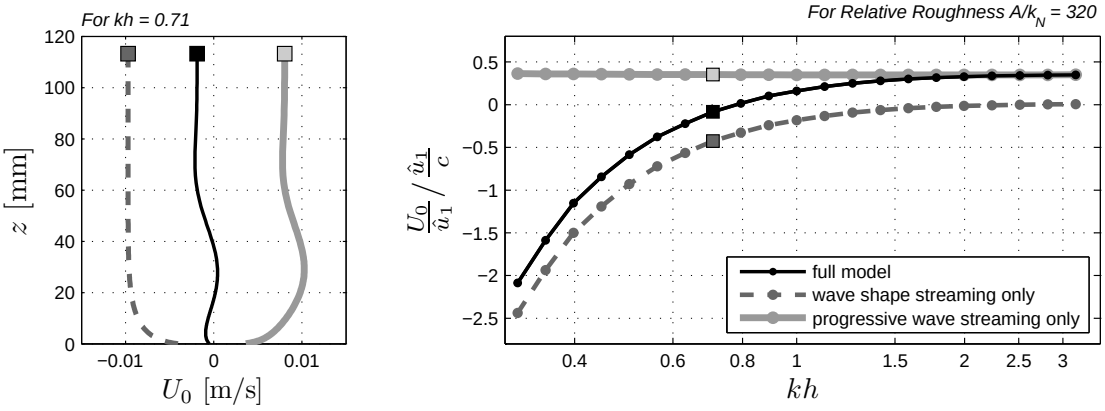

Figure 4. Streaming velocities from full model simulations (black), simulations with wave shape effect only (gray / dashed line), and progressive wave effect only (light gray); Left) streaming profiles for a single kh-value; right) non-dimensional streaming at the outer edge of the boundary layer as function of relative water depth kh (on log-scale) for $A/k_N = 320$.

bed shear stress (Meyer-Peter and Müller type) as hydrodynamic input (e.g. Van Rijn (2007), (Nielsen (2006)). The results for the streaming at the top of a rough turbulent boundary layer can be parameterized as follows:

$$\frac{U_0 / \hat{u}_1}{\hat{u}_1 / c} = 0.345 + 0.7\left(\frac{A}{k_N}\right)^{-0.9} - \frac{0.25}{\sinh^2(kh)} \quad \text{or} \quad \frac{U_0}{\hat{u}_1} = 0.345\frac{\hat{u}_1}{c} + 0.7\left(\frac{A}{k_N}\right)^{-0.9}\frac{\hat{u}_1}{c} - \frac{2}{3}\left(R - \frac{1}{2}\right) \qquad (5)$$

In these parameterizations, the first two terms are connected to progressive wave streaming and the last term to wave shape streaming, with parameter $R = u_{max} / (u_{max} - u_{min})$ describing the velocity skewness. Especially the latter is convenient to estimate the importance of the two streaming process for a measured velocity signal.

4. Results (II): Sediment Transport

4.1. *Validation results*

Before we can use the model to determine the contribution of progressive wave streaming to sediment transport, we need to validate the model's sediment transport predictions. Hereto, both tunnel and flume experiments on transport of both fine and medium sized sand have been simulated with the model. The validation cases with oscillatory flow originate from Ribberink & Chen (1993), Ribberink & Al-Salem (1994), Ribberink & Al-Salem (1995), Wright (2002) and O'Donoghue & Wright (2004). The flume cases stem from Dohmen-Janssen & Hanes (2002) (set 'Flume (I)', medium sized sand only) and Schretlen

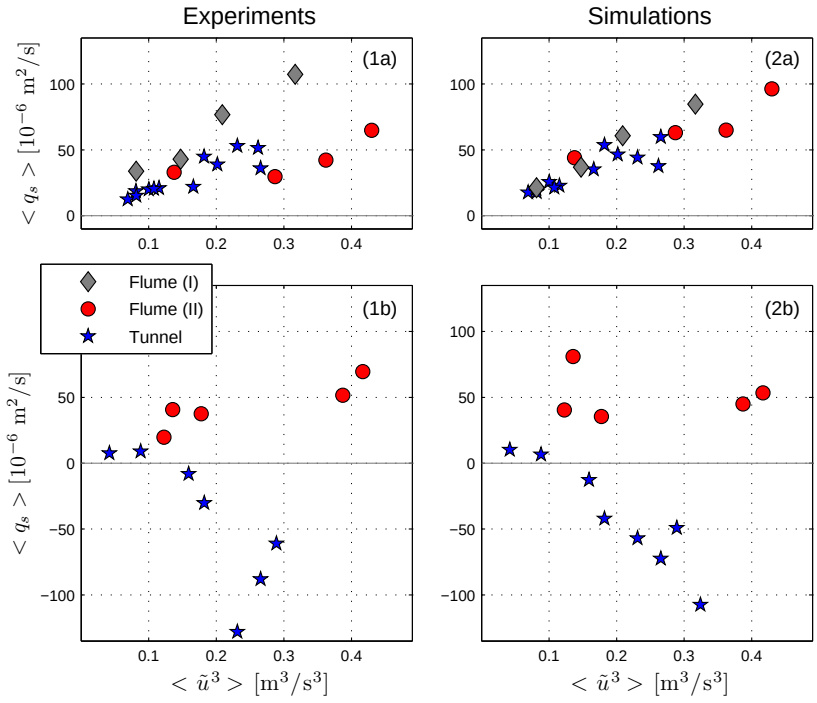

Figure 5. Measured (1a,b) and computed (2a,b) net sediment transport rates $<q_s>$ of medium (panels a) and fine (panels b) sands against the third order velocity moment determined from the oscillating part of the horizontal velocity $\tilde{u}$, for various experimental conditions from both tunnel and flume experiments.

(2012) (set 'Flume (II)', both medium and fine sized sand). To simulate the experiments, the model – either in tunnel or flume version – is forced with the measured velocity signals, which for all these cases are predominantly velocity-skewed. We refer to Kranenburg et al. (2013) for a complete overview of the validation cases.

A direct comparison of measured and computed sediment transport rates showed that the model's under- or overprediction of the experimentally determined transport rates was on averaged within a factor 1.4. Rather than this direct comparison, we show here a – more informative – comparison on trends (Figure 5). An important observation from tunnel experiments with velocity skewed oscillatory flows is that the net transport rate of medium sized sand ($d_{50} \geq 0.2$ mm) is proportional to the third-order moment of the horizontal orbital velocity in the free stream: $<q_s> \sim <\tilde{u}^3>$ (Ribberink & Al-Salem, 1994) (see panel 1a). This relation, an indication for quasi-steady behavior of $<q_s>$ during the wave cycle, is not valid for finer sands (O'Donoghue & Wright, 2004). In that case, phase-lag effects will play a role and net transport rates can even become negative for increasing positive velocity moments $<\tilde{u}^3>$ (see panel 1b). In wave flume experiments, the $<q_s> \sim <\tilde{u}^3>$ relation for medium sized sand is also found (Dohmen-Janssen & Hanes, 2002) (see panel 1a). However, the reversal of transport direction for fine sand is absent (Schretlen, 2012) (see panel 1b). Panel 2b clearly shows that the different trends in transport of fine sand between for tunnel and flume experiments are well reproduced by the model. Also the moment of transition from onshore to offshore transport for fine sand ($<\tilde{u}^3> \approx 0.15$ m^3/s^3) is predicted correctly. Panel 2a shows that, like in the experiments, the simulated transport rates of medium sized sand are generally increasing with increasing $<\tilde{u}^3>$. A remarkable observation is that the increased onshore transport of medium sized sand in the flume compared to the tunnel experiments as observed by Dohmen-Janssen & Hanes (2002) is not present in the data of Schretlen (2012). This might be due to the wide sieve curve of the sand in the latter experiment.

4.2. *Results of model research on the importance of Progressive Wave Effects for net sediment transport*

Next we carry out further model tests to determine the contribution of progressive wave streaming to sediment transport. Hereto, test conditions have been defined with a constant wave period T (6.5s) and water depth h (3.5m), but gradually increasing wave height H (0.7-1.6m). In these tests, the fluctuating part of the near bed free stream horizontal velocity is determined from T, h and H with the Fourier approximation method of Rienecker & Fenton (1981). This results in velocity signals with increasing velocity skewness and increasing third order velocity moment $<\tilde{u}(t)^3>$ for increasing H. For the defined test

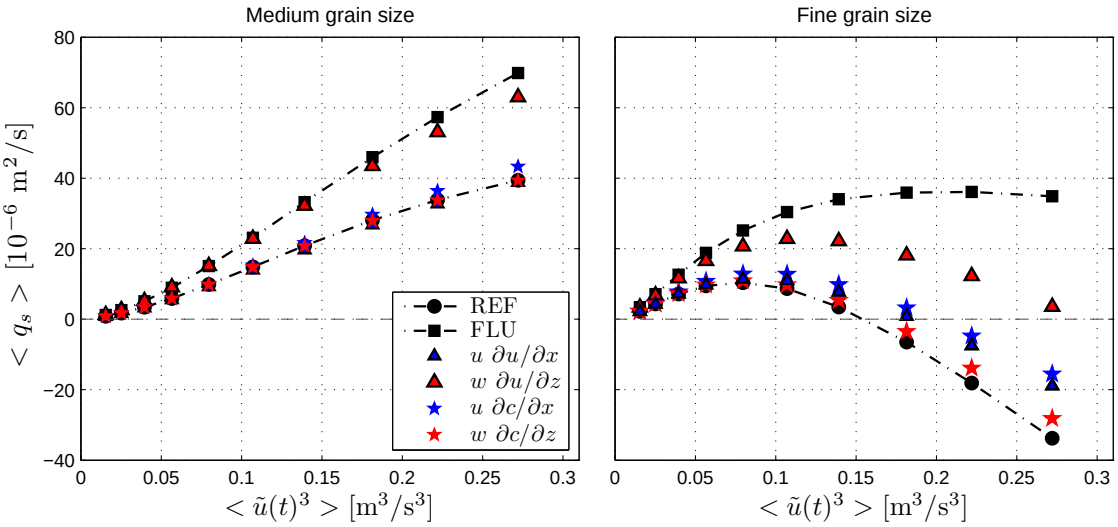

Figure 6. Net transport rates $<q_s>$ of medium (0.25mm) and fine (0.14mm) sized sediments for velocity skewed waves with increasing wave height, here plotted against $<\tilde{u}^3>$. The figure shows results obtained with all advective terms switched on (FLU), all advective terms switched off (REF), and only $w\partial u/\partial z$, $w\partial c/\partial z$, $u\partial c/\partial x$ or $u\partial u/\partial x$ switched on.

cases, we simulate the sediment transport with all advective terms switched on (FLU, because it models the flume situation), with all advective terms switched off (REF), and with only $w\partial u/\partial z$, $w\partial c/\partial z$, $u\partial c/\partial x$ or $u\partial u/\partial x$ switched on individually. Note that $w\partial u/\partial z$ is the term in the momentum equation that induces the progressive wave streaming.

Figure 6 shows transport rates computed with the defined input for both medium (d_{50}=0.25 mm) and fine sized sediment (d_{50}=0.14 mm), plotted against the third order velocity moment. The results provide insight in the relative importance of individual advective processes in explaining the differences between tunnels and flumes, and show how the relative contribution of the various terms changes with changing wave and bed conditions. Figure 6 shows that progressive wave streaming, induced by $w\partial u/\partial z$, indeed contributes substantially to onshore sediment transport. For the medium grains almost the complete difference between flume (FLU) and tunnel (REF) simulations is covered when the vertical momentum advection term $w\partial u/\partial z$ is taken into account. However, in case of fine sand, with higher volumes of sediment in suspension, also the divergence and convergence in horizontal advection becomes important, especially $u\partial c/\partial x$. The figure also shows that the relative contribution of this term increases with increasing wave height.

The background of this fine sand transport mechanism is illustrated in Figure 7, showing the surplus of the sediment concentration resulting from this term for a simulation with a sinusoidal forcing. The horizontal gradients in the sediment flux cause an accumulation of sediment in front of the wave top, where the flux gradient $\partial(uc)/\partial x < 0$. Behind the top the opposite occurs. As a result, the absolute rates of change of the sediment concentration are larger and the concentration reacts faster on velocity changes during onshore flow than during offshore flow. A modulation in the concentration takes place, with an amplification of the concentration peak at maximum onshore velocity and a reduction at maximum offshore velocity, see (panel b). Multiplied with the flow velocity, this modulation in sediment concentration induces a net contribution to sediment transport in onshore direction. Figure 7 also shows the result of sediment advection by the vertical orbital motions under progressive waves (panel a). During the off- to onshore flow reversal, this motion will be upward. At the reversal from on- to offshore, it will be downward. As a result under the crest more sediment is present at higher levels, under the trough more sediment is present near the bed. Consequently, an offshore net sediment flux appears higher up in the boundary layer and an offshore net sediment fluxes appears near the bed. These opposite contributions finally lead to a relatively small influence of vertical sediment advection on the vertically integrated net flux or net transport rate (panel c).

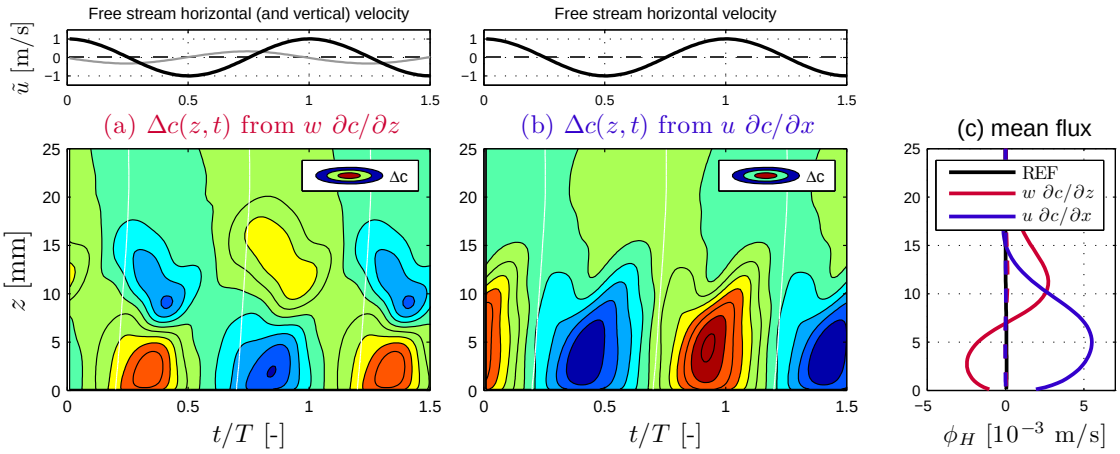

Figure 7. Surplus of the sediment concentration induced by the advective terms w$\partial c/\partial z$ and $u\partial c/\partial x$ with their consequence for the mean sediment flux (panel c). REF: reference simulation with all advective terms switched off. Solid lines: total wave averaged sediment flux $\underline{uc}$; The top panels show free stream velocities. The white lines in (a) and (b) indicate flow reversal. Condition: sinusoidal wave with T = 6.5s, $\hat{u}$ = 1.0m/s, h = 3.5m, d_{50} = 0.1mm.

4.3. *Parameterization*

The effect of diverging / converging horizontal advection is not included in present day sediment transport formulas, or it is assumed to be strongly correlated to the streaming effect (Nielsen, 2006). The results above show that the effect of the divergence/convergence and its contribution relative to the other progressive wave effects is strongly grain size dependent. Next, we saw that the process actually causes an adaptation of the reaction speed of the concentration on changing velocities. It can therefore be seen as a process affecting the – grain size dependent – phase-lag effect.

The phase-lag effect has been included in some transport formulas through a phase-lag parameter T_a/T, i.e. the settling time relative to the wave period, with T_a the stirring height δ devided by settling velocity w_s (Dohmen-Janssen et al., 2002). We propose to include the horizontal advection affect through an adaptation of this phase lag parameter, with the following expression for T_a:

$$T_a(t) = \frac{\delta}{w_s}\left\{1 - \frac{\alpha u_\infty(t)}{c_p}\right\} \tag{6}$$

Here c_p is the wave propagation speed, u_∞ the free stream velocity and $\{1\text{-}\alpha u_\infty/c_p\}$ is < 1 during onshore flow and > 1 during offshore flow. To see its effect, consider a simple transport formula that expresses the depth integrated sediment flux q_s as function of the free stream velocity u_∞ and the depth-averaged volume concentration $C(t)$:

$$q_s(t) = \int_{z=zbed}^{zbed+\delta} ucdz = \alpha\delta u_\infty(t) C(t) \tag{7}$$

with δ the thickness of the layer over which transport (and averaging) takes place and α a distribution coefficient related to the shape of the concentration and velocity profiles (O(1)). The time-dependent behavior of the depth-averaged concentration $C(t)$ in gradually-varying flows can be represented in a schematic way by a relaxation equation:

$$\frac{\partial C(t)}{\partial t} = \frac{\gamma\{C_{eq}(t) - C(t)\}}{T_a} \tag{8}$$

with T_a the relaxation time scale of adaptation of the sediment concentration to the equilibrium concentration C_{eq}, and γ a coefficient related to the shape of the concentration profile. The (depth-averaged) C_{eq} reflects the 'carrying capacity' of the flow: the concentration for which the sediment settling and pick-up are equal, which is directly related to the instantaneous forcing.

In combination with (8), the parameterization of equation (6) introduces the increasing phase-lag between velocity and concentration for decreasing grain size. For velocity-skewed oscillatory flow ('infinite' c_p), this will lead to net offshore transport when combined with the simple transport formula of equation (7). Next, and that is the key element, the parameterization of equation (6) reflects the behavior of the concentration under progressive waves: (1) the concentration will adapt faster during the onshore motion than during the offshore motion, (2) increased/decreased maximum concentration will be found under the wave crest/trough, and (3) the advection effects will increase with decreasing grain size. Combined with equation (7), this leads to additional onshore transport.

Here we discussed the parameterization starting from intra-wave velocities and formulas for time-dependent concentration and sediment transport. However, the principle can equally well be implemented in transport formulas based on the half-wave approach, applying a single separate value for the adaptation time during on- respectively offshore motion, as only the maximum and minimum velocity are used to characterize the wave.

5. Discussion: Morphology

The results of section 4 show the importance of progressive wave effects for sediment transport. Next, we discuss the implications of our results for morphological modeling. Hereto, we carry out an explorative computation of sand bar migration both with and without progressive wave effects.

We consider a cross-shore profile with a single sand bar around 200 m offshore (Figure 8, panel a). The profile is affected by three days of wave action of perpendicular incident, steady waves (period T = 5.0 s, height H = 0.8 m at 450 m offshore where water depth h = 6.3 m). The chosen profile and wave conditions are based on the situation on 24-26 September 1994 near Duck, NC, USA (Gallagher, Elgar, & Guza, 1998), where onshore bar migration was observed. For these conditions, the near-bed flow in the bar area will be large enough to generate sheet-flow, while the waves will not break at the bar and the return current influence will be limited.

Firstly we calculate the wave height along the profile with a shoaling computation starting at 6.3 m water depth. For simplicity, energy loss from bottom friction is neglected and waves are assumed to break as soon as the wave height / water depth ratio exceeds 0.65 (Figure 8, around x = -80 m). Secondly, the wave-related near-bed free stream velocity along the profile is again calculated from the T, H and h using 2nd order Stokes theory. Next, for a selection of 24 cross-shore locations between x = -450 and x = -100 m, simulations are carried out with the model of this study using the calculated near-bed velocity signal as forcing. These model runs result in values for the wave-averaged sediment transport rates $<q_s>$ at these locations. The results are interpolated (using splines and a fine x-grid) to obtain sediment transport rates along the profile from 450 till 100 m offshore (Figure 8, panel b, the dots are model results). Subsequently, profile changes are calculated from the convergence / divergence of sediment transport during time

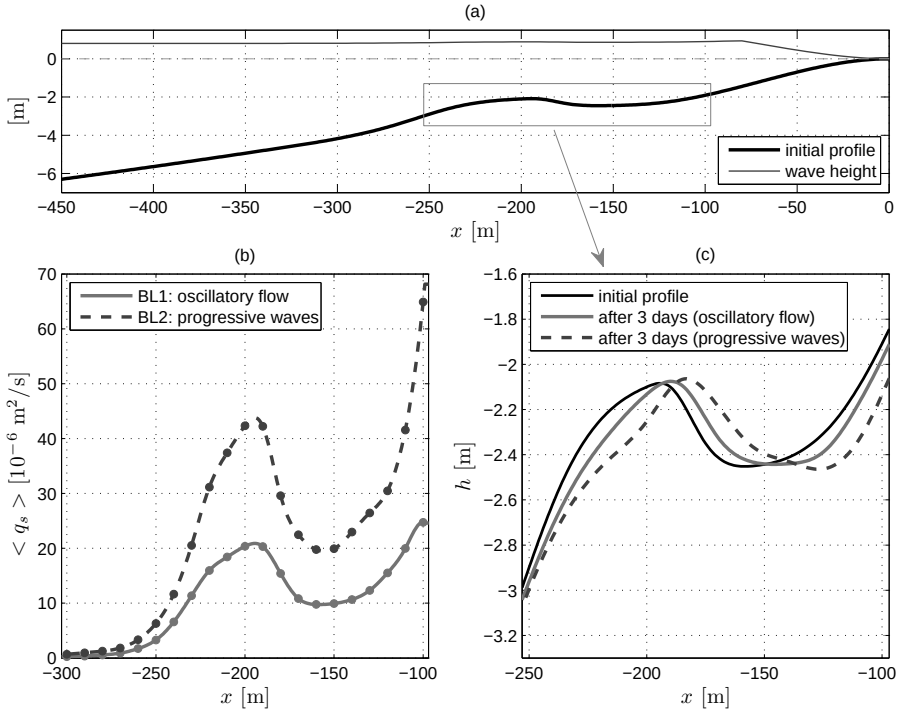

Figure 8. Morphodynamic example: computation of the development of a cross-shore profile using the process-based numerical model either with (BL2) or without (BL1) progressive wave effects. (a) initial bed level and wave height; (b) wave averaged sediment transport rates $<q_s>$ during the first time step; (c) resulting bed levels around the sandbar after 3 days, all plotted against the cross-shore position. Condition: T = 5.0s, H = 0.8m at 6.3m water depth, d_{50} = 0.20mm.

intervals of ½ an hour. After updating the bed profile, new transport rates are determined for the selected cross-shore locations. However, rather than running new computations / simulations for hydrodynamics and sediment transport, this is done using the old simulation results: because energy loss from friction was neglected and no memory for wave shape deformation is present in the used wave theory, every water depth is connected to a single wave height and wave shape and therefore to a single results for the transport rate. Hence, the transport rates belonging to the new bed levels / water depths can be determined from interpolation between the earlier computed $<q_s>$-values. In this way profile changes are computed till three days have passed (144 time steps). We carry out this procedure using the model of section 2 both with (BL2) and without (BL1) progressive wave effects. The resulting bed levels around the sandbar are shown in (Figure 8, panel c).

We conclude from the figure that either or not including progressive wave effects in morphodynamic predictions can result in large differences in the predicted sandbar migration. In this example, the difference in predicted migration speed of the sandbar crest with and without progressive wave effects is a factor 2. Note that for finer sized sand, e.g. d_{50} = 0.15 mm, larger differences and even opposite migration directions may be expected, with offshore migration when progressive wave effects are neglected. Notwithstanding the strong simplifications in this morphological model and the absence of validation with measurements, we believe the large difference in migration rate is an important observation.

Present day morphodynamic models do not or only limitedly account for progressive wave effects. At the same time they tend to under predict onshore transport in accreting conditions (see e.g. Gallagher et al. (1998), Van Rijn et al (2011)). Together, these issues further underline the necessity to properly accounting for progressive wave effects in morphodynamic models. Hereby, it is not realistic and also not needed to use a detailed boundary layer model as applied in this study within the context of a morphological model. A more feasible way is to improve the way existing sediment transport formulas presently applied within morphological models account for progressive wave effects. For this, the parameterizations developed within this study are useful building blocks.

6. Conclusion

Compared to oscillatory flow, progressive waves cause more sediment to be transported in onshore direction. Progressive wave streaming explains the major part of this difference. However, especially for fine sand, also an additional variation in the sediment concentration under progressive waves contributes significantly. These mechanisms should be accounted for in sediment transport formulas within morphological models. The parameterizations of het numerical model results from this study form useful building blocks hereto.

Acknowledgements

The authors acknowledge Rob Uittenbogaard (Deltares), Hydralab IV-WISE (EU) and SANTOSS (EPSRC/STW).

References

Campbell, L. J., O'Donoghue, T., & Ribberink, J. S. (2007). Wave boundary layer velocities in oscillatory sheet flow. In J. McKee Smith (Ed.), *Proceedings of 30th International Conference on Coastal Engineering* (pp. 2207-2219). San Diego, California, USA, 2006: World Scientific Publishing.

Dohmen-Janssen, C. M., & Hanes, D. M. (2002). Sheet flow dynamics under monochromatic nonbreaking waves. *Journal of Geophysical Research, 107*(C10), 1-21. doi:10.1029/2001JC001045

Dohmen-Janssen, C. M., Kroekenstoel, D. F., Hassan, W. N., & Ribberink, J. S. (2002). Phase lags in oscillatory sheet flow: experiments and bed load modelling. *Coastal Engineering, 46*(1), 61-87. doi:10.1016/S0378-3839(02)00056-X

Gallagher, E. L., Elgar, S., & Guza, R. T. (1998). Observations of sand bar evolution on a natural beach. *Journal of Geophysical Research, 103*(C2), 3203-3215.

Klopman, G. (1994). *Vertical structure of the flow due to waves and current*. Progress report, H840.30, Part II, Delft, The Netherlands.

Kranenburg, W. M., Ribberink, J. S., Schretlen, J. J. L. M., & Uittenbogaard, R. E. (2013). Sand transport beneath waves: The role of progressive wave streaming and other free surface effects. *Journal of Geophysical Research: Earth Surface*, *118*, n/a-n/a. doi:10.1029/2012JF002427

Kranenburg, W. M., Ribberink, J. S., Uittenbogaard, R. E., & Hulscher, S. J. M. H. (2012). Net currents in the wave bottom boundary layer: on wave shape streaming and progressive wave streaming. *Journal of Geophysical Research*, *117*(F03005). doi:10.1029/2011JF002070

Longuet-Higgins, M. S. (1953). Mass transport in water waves. *Philosophical Transactions of the Royal Society of London. Series A, Mathematical and Physical Sciences*, *245*(903), 535-581.

Nielsen, P. (2006). Sheet flow sediment transport under waves with acceleration skewness and boundary layer streaming. *Coastal Engineering*, *53*(9), 749-758. doi:10.1016/j.coastaleng.2006.03.006

O'Donoghue, T, & Wright, S. (2004). Flow tunnel measurements of velocities and sand flux in oscillatory sheet flow for well-sorted and graded sands. *Coastal Engineering*, *51*(11-12), 1163-1184. doi:10.1016/j.coastaleng.2004.08.001

Ribberink, J. S., & Al-Salem, A. A. (1994). Sediment transport in oscillatory boundary layers in cases of rippled beds and sheet flow. *Journal of Geophysical Research*, *99*(C6), 12707-12727.

Ribberink, J. S., & Al-Salem, A. A. (1995). Sheet flow and suspension of sand in oscillatory boundary layers. *Coastal Engineering*, *25*(3-4), 205-225. doi:10.1016/0378-3839(95)00003-T

Ribberink, J. S., & Chen, Z. (1993). *Sediment transport of fine sand under asymmetric oscillatory flow*. Report, Delft, The Netherlands.

Ribberink, J. S., van der Werf, J. J., O'Donoghue, T., & Hassan, W. N. M. (2008). Sand motion induced by oscillatory flows: Sheet flow and vortex ripples. *Journal of Turbulence*, *9*(20), 1-32. doi:10.1080/14685240802220009

Richardson, J. F., & Zaki, W. N. (1954). Sedimentation and fluidisation: Part I. *Transactions of the Institution of Chemical Engineers*, *32*, S82-S100. Institution of Chemical Engineers. doi:10.1016/S0263-8762(97)80006-8

Rienecker, M. M., & Fenton, J. D. (1981). A Fourier approximation method for steady water waves. *Journal of Fluid Mechanics*, *104*, 119-137.

Schretlen, J. L. M. (2012). *Sand transport under full-scale progressive surface waves* (p. 156). PhD-thesis, University of Twente, Enschede, The Netherlands.

Trowbridge, J., & Madsen, O. S. (1984). Turbulent wave boundary layers 2. Second-order theory and mass transport. *Journal of Geophysical Research*, *89*(C5), 7999-8007.

Van Rijn, L. C. (1993). *Principles of sediment transport in rivers, estuaries and coastal seas*. Amsterdam, The Netherlands: Aqua Publications.

Van Rijn, L.C., Tonnon, P. K., & Walstra, D. J. R. (2011). Numerical modelling of erosion and accretion of plane sloping beaches at different scales. *Coastal Engineering*, *58*(7), 637-655. Elsevier B.V. doi:10.1016/j.coastaleng.2011.01.009

Van Rijn, Leo C. (2007). Unified view of sediment transport by currents and waves. I: Initiation of motion, bed roughness, and bed-load transport. *Journal of Hydraulic Engineering*, *133*(6), 649. doi:10.1061/(ASCE)0733-9429(2007)133:6(649)

Wright, S. (2002). *Well-sorted and graded sand is oscillatory sheet-flow* (p. 207). Aberdeen: PhD-thesis University of Aberdeen, UK.